

The diffuseness of low-mass galaxies in the FIREbox simulation

by
Marckie Zeender

Professor Moreno, Advisor

A thesis submitted in partial fulfillment
of the requirements for the
Degree of Bachelor of Arts with Honors
in Physics



Claremont, California
April 2, 2023

Abstract

Executive Summary

Acknowledgments

To Profe Moreno for reading my draft

Contents

Abstract	i
Executive Summary	ii
Acknowledgments	iii
1 Introduction	1
1.1 Physical models	1
1.2 Low-mass galaxies and their tensions	2
1.3 @Profe Moreno, should delete this section, or should I rewrite it?	2
1.4 Tension in the size-mass relation	4
1.5 FIREbox Galaxy Simulation	4
2 Methods	6
2.1 The Data	6
2.2 The Diffuseness Parameter	7
2.3 Proximity	10
2.3.1 Minimum Proximity	10
3 Results and discussion	11
3.1 Diversity of Dwarf Diffuseness	11
3.2 Proximity to Host Galaxy	11
3.3 Minimum Proximity	12
3.4 Proximity to Nearest Neighbor	12
4 Conclusions and future work	15
4.1 Size-mass-proximity relation	15
4.2 Further Work	16
A Calculating distances in FIREbox	18

List of Figures

- | | | |
|-----|---|---|
| 1.1 | From: Sales et al. (2022). A comparison of the sizes and masses of dwarf galaxies from simulations and reality. The y axis plots r_{50} and the x axis plots M_{50} . The gray squares depict real galaxies from the Milky Way's local group, whose data was compiled by McConnachie (2012). The other colors depict data from various simulations other than FIREbox. As we can see, the dwarfs from the local group show much diversity in their size-mass ratios. The simulated galaxies, however, show more consistency, especially when compared to others from their own simulation (for example, notice that the orange circles are all clustered together). | 3 |
| 1.2 | A comparison the size and detail of cosmological simulations. There is a tradeoff between scale and resolution, where a total increase in both means a higher dynamic range at the cost of computer performance. FIREbox has the highest dynamic range, and therefore the highest computational cost. | 5 |
| 2.1 | From: Feldmann et al. (2022). A representation of the FIREbox simulation. The first two rows depict the state of the simulation at three different time points; the rightmost images depict the simulation in the present time. The top row depicts dark matter in blue and stellar matter in white, while the middle row depicts gas. The bottom row shows a galaxy at different scales within a cluster. As we can see, matter collects into galaxies and systems of galaxies over the course of the simulated universe's evolution. These galaxies take on a variety of sizes, and they share threads of gas and are contained within hierarchical halos of dark matter. | 8 |
| 2.2 | The left shows the size-mass relationship for the FIREbox dwarf galaxies. It covers the range $3 \cdot 10^3 - 10^9$. Galaxies larger than this are no longer dwarfs and do not follow the power law, and galaxies smaller than this approach FIREbox's resolution limit. The line of best fit is described by equation 2.2 and β represents the deviation from that line. β is chosen to characterize the diffuseness of a galaxy because the distribution of β is essentially independent of mass, which can be seen in on the right. | 9 |

- | | | |
|-----|--|----|
| 3.1 | Shows the diffuseness of satellites as a function of distance to their host galaxies. On the left, it compares the absolute separation. On the right, it shows the Virial separation (distance as a fraction of the host galaxy's Virial radius). The correlation for these is small: $r = .22, p \leq .001$ for d and $r = .26, p \leq .001$ for d/R_{vir} . This slight positive correlation in both sets of parameters is likely caused by the dark matter deficient galaxies (shown in light green and yellow), whose outer regions are likely tidally disrupted, leaving only a core. | 12 |
| 3.2 | Shows the diffuseness of satellites as a function of minimum distance to their host galaxies. On the left, it compares the absolute separation. On the right, it shows the Virial separation. There is no correlation for these parameters: $r = .04, p = .51$ for d_{min} and $r = -0.07, p = .25$ for d_{min}/R_{vir} | 13 |
| 3.3 | A zoom-in of figure 3.2 showing the diffuseness of satellite galaxies as a function of their minimum Virial separation. This graph only includes galaxies above the critical separation of $0.2R_{vir}$, below which a galaxy would either be entirely destroyed or converted into a dark matter deficient galaxy. There is a medium negative correlation between these parameters: $r = -0.32, p \leq .001$ | 13 |
| 3.4 | Shows a galaxy's distance to its nearest neighbor. There is a slight negative correlation between these parameters: $r = .26, p \leq .001$. We | 14 |

Chapter 1

Introduction

Understanding the composition and structure of galaxies, and the role that dark matter plays in their organization, is a pressing topic in modern cosmology. A common method to explore these questions is using numerical simulations. This approach allows us to choose plausible initial conditions and laws of physics in order to test how the universe would behave under those conditions. We can then compare those results to real-world observations to determine the accuracy of those physical assumptions. For instance, if we wanted to test Newton’s theory of gravity in our solar system, we could run a numerical simulation of Newton’s equation using a known initial position of the planets, and test whether the simulated motion of the planets aligns with reality. Likewise, we can test our theories about dark matter and gravity by running cosmological simulations.

1.1 Physical models

Our current leading theory for dark matter’s role in galaxy evolution is the cosmological constant plus cold dark matter (Λ CDM) model (Sales et al., 2022). This theory provides a framework for cosmological simulations that incorporates a non-interacting model for dark matter and the cosmological constant model of dark energy. The “cold” dark matter model means that we assume that dark matter particles interact with neither each other nor “normal” baryonic matter, except through gravity. This is in contrast to other competing theories such as superfluid dark matter, which interacts with itself to form a superfluid (De Luca and Khouri, 2023). These dark matter models predict large dark matter halos around galaxies (Feldmann et al., 2022), which is consistent with observations of gravitational lensing—visual distortions due to gravity. Not much is known about dark matter beyond its gravitational effects on baryonic matter, and we have yet to find a non-gravitational interaction between these two.

The Λ CDM assumes dark energy to be the cosmological constant Λ , which is a degree of freedom in the Einstein Equation that adds a net offset to the energy density of a vacuum. However, there are alternative theories of dark energy; Bassi et al. (2023) shows that the Bimetric gravity model could also explain the effects of dark energy. If more evidence can be

found in support of these alternative models, then Bimetric and/or superfluid dark matter may replace Λ CDM as the leading cosmological model.

When creating a cosmological simulation, astrophysicists must also incorporate baryonic processes, the physics of ordinary matter. These processes include chemistry, thermal physics, and the formation, evolution, and feedback of stars. Our current computers limit us such that we cannot resolve individual stars within galaxies (Feldmann et al., 2022) because there are simply too many, and stellar physics at these scales is not fully understood. Earlier simulations, such as Bournaud et al. (2010), were forced to ignore stellar processes entirely in favor of gaseous ones. They found that the simulated galaxies grew too massive and cooled too quickly compared to real galaxies. This tension was resolved by the creation of the Feedback in Realistic Environments (FIRE) physics model (Hopkins et al., 2018). FIRE adopts a subgrid model that simulates large chunks of matter (referred to as particles), each containing many stars. It then uses the estimated number of stars in each particle to simulate stellar feedback.

1.2 Low-mass galaxies and their tensions

Until recently, low-mass “dwarf” galaxies have not been closely studied due to them being difficult to detect with telescopes. For a period of time, the Λ CDM model was questioned because it predicted the existence of many more dwarf galaxies than had been observed in the region around the Milky Way (Sales et al., 2022). According to Sales et al. (2022), enough dwarf galaxies have been discovered in recent years to resolve this tension. However, the sudden influx of dwarf galaxy observations has provided astrophysicists number of new tensions. The diversity of the size-mass relation of dwarf galaxies is one such tension. Observational data of dwarf galaxies near the Milky Way suggests that the correlation between the mass and size of satellite dwarf galaxies is not as strong as simulations seem to predict (Sales et al., 2022).

1.3 @Profe Moreno, should delete this section, or should I rewrite it?

It is a common myth that if we can simulate something, we must be able to fully understand it. Unfortunately, this is not generally true. The galaxy simulations we use are so complex and detailed that it is often very difficult to determine what physical assumptions or initial conditions cause certain behaviors. While it is much easier to make collect data from simulations—we do not need telescopes and we can view the galaxies in 3D with arbitrary resolution—we must still analyze that data using similar techniques used to study real galaxies.

If it is demonstrated that one of these tensions is caused by neither numerical approximations in the simulations nor simplifications of baryonic physics, then it could call the Λ CDM

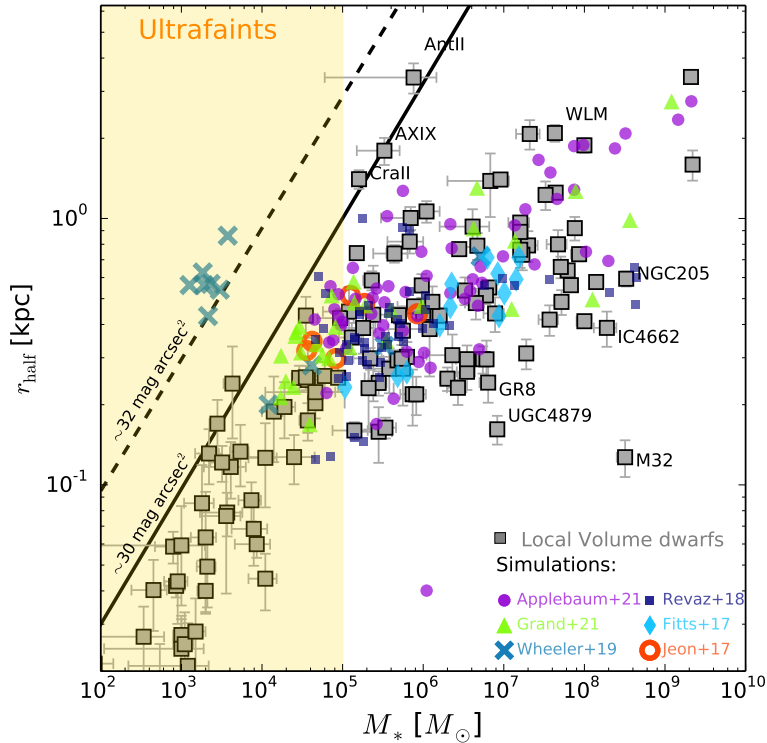


Figure 1.1: From: Sales et al. (2022). A comparison of the sizes and masses of dwarf galaxies from simulations and reality. The y axis plots r_{50} and the x axis plots M_{50} . The gray squares depict real galaxies from the Milky Way's local group, whose data was compiled by McConnachie (2012). The other colors depict data from various simulations other than FIREbox. As we can see, the dwarfs from the local group show much diversity in their size-mass ratios. The simulated galaxies, however, show more consistency, especially when compared to others from their own simulation (for example, notice that the orange circles are all clustered together).

model into question.

1.4 Tension in the size-mass relation

The observed dwarf galaxies near the Milky Way have widely varying radii compared to their masses. In other words, both diffuse and compact dwarf galaxies are relatively common. However, galaxy simulations including Fitts et al. (2017) tend to form galaxies with much stricter size-mass ratios (Sales et al., 2022). Some may argue that these discrepancies are caused by numerical inaccuracy. However, even the simulations with the highest numerical resolution such as Wheeler et al. (2019) lack diversity in size-mass ratios for dwarf galaxies.

The diversity of sizes of dwarf galaxies must therefore be caused by something else. Tidal disruption could be the answer. When a dwarf galaxy passes by a larger galaxy, its dark matter halo can be destroyed by the tidal force exerted on it, according to Moreno et al. (2022). This can also lead to the creation of an ultra-compact dwarf (Applebaum et al., 2021), because the galaxy will lose its outer regions. It is therefore plausible that close interactions between galaxies is what causes variance in size.

1.5 FIREbox Galaxy Simulation

Scale and resolution are important for simulations. Astrophysicists must balance large volume and high detail, both of which cost computing power. The large volume simulations allow us to closely study intergalactic systems and to collect large amounts of statistical information about galaxies (Feldmann et al., 2022). However, a higher resolution “zoom in” simulation such as FIRE in the Field (Fitts et al., 2017) allows us to better simulate the internal physics of the galaxies themselves.

This paper will examine data from FIREbox (Feldmann et al., 2022). This cosmological simulation does not have the largest volume, nor is it the most detailed. Rather, it incorporates a balance of high detail and large scale (see figure 1.2), which together give it the highest dynamical range of any cosmological simulation to this date.

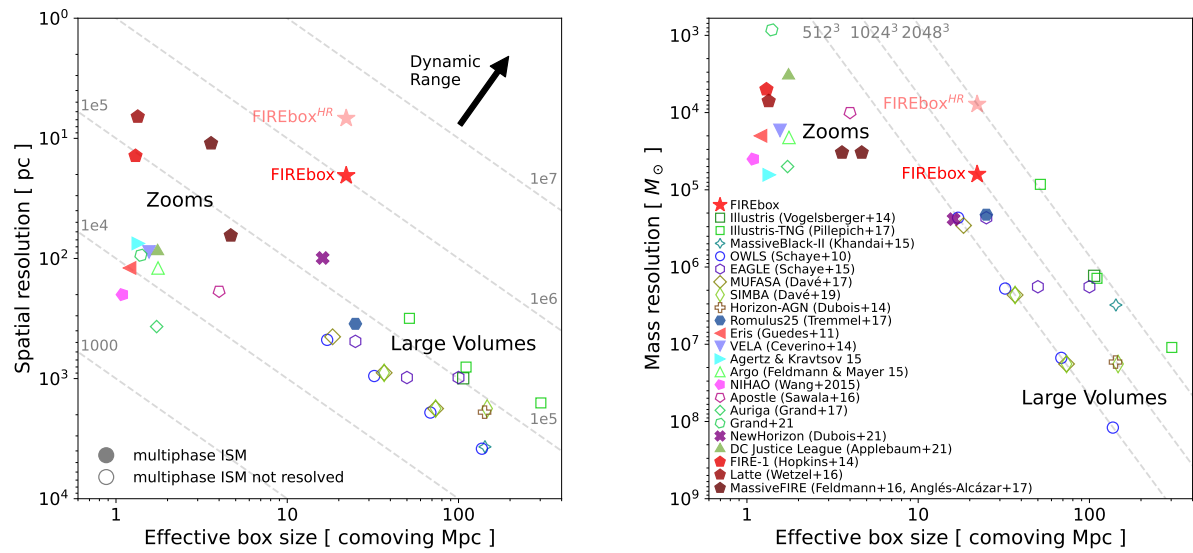


Figure 1.2: A comparison the size and detail of cosmological simulations. There is a tradeoff between scale and resolution, where a total increase in both means a higher dynamic range at the cost of computer performance. FIREbox has the highest dynamic range, and therefore the highest computational cost.

Chapter 2

Methods

2.1 The Data

Over the course of the evolution of the FIREbox simulation, 1201 snapshots of the state of the universe were collected (Feldmann et al., 2022). They were approximately evenly spaced out in time and included the positions of the particles, their densities, metallicities, star-formation rates, and other properties. The particle data was reduced by grouping the particles into their respective galaxies and dark matter halos. They used the AMIGA Halo Finder (AHF; Knollmann and Knebe (2009)) to sort the halos into categories of halos and sub-halos, which in turn allowed them to categorize the galaxies by host and satellite galaxies respectively. The reduced data, known as the galaxy and halo catalog, includes galaxy information such as position, radius, mass and star formation rate, as well as data about the dark matter halos around those galaxies. For the extent of this experiment, we will be using the snapshot 1201, the final state of the simulation. This snapshot depicts the simulated present day.

Each parameter for the galaxies is split between a few different definitions. For the purpose of this experiment, we will use the following definitions unless otherwise specified. The galaxy's radius R_{50} is defined to be the radius that contains 50% of its stars, as determined by AHF. The galaxy's mass M_* is defined to be the mass of the stars contained within R_{50} . We are not going to include dark matter in this definition. The reader should note that this is not the only way to define these parameters. Due to the fluid nature of matter on a galactic scale, it is often arbitrary as to whether a given particle belongs to a given galaxy. Alternate definitions include different thresholds for the radius, such as R_{80} , and different kinds of matter included in the mass, such as gas matter and dark matter.

Other parameters that we will use are a galaxy's position in space and its flyby distance—a satellite galaxy's minimum distance to its host galaxy. All distances (including radius) are measured in terms of the co-moving parameter h , a time-dependent scaling factor of the universe. In the final state of FIREbox, $h = 0.6774\text{kpc}$.

McConnachie (2012) compiled a number of data sets for dwarf galaxies in the local group of the Milky Way. One data set includes the galaxies' radii and another contains their mass. The radius is defined slightly differently in this case. It is the half-light radius, the

radius from which half of the galaxy's light is emitted. The mass parameter is calculated by assuming a mass-light ratio of one, meaning that the brightness per unit mass is equal to the Sun. For the sake of this experiment, we will assume that the half-light radius is equal to R_{50} the presumed M_* is equal to M_* . To get this data in a usable form, I first dumped the text-based datasets into pandas spreadsheets. I removed invalid rows and then merged them by galaxy name. For galaxies whose names were reported differently on the different sheets, I merged them by hand. I then cast the mass and radius to float64 for use in the analysis.

2.2 The Diffuseness Parameter

As diffuseness will be main subject of this paper, let us define it. The dwarf galaxies in FIREbox loosely follow a power law size-mass relationship (see figure 2.2). The relationship can therefore be described using the following equation.

$$\frac{R_{50}}{1kpc} \approx a \left(\frac{M_*}{M_\odot} \right)^\gamma \quad (2.1)$$

Where γ and a are constants and M_\odot is the mass of the sun. We are dividing by a kiloparsec unit to make the equation unitless. Taking the logarithm of this equation gives us

$$\ln \left(\frac{R_{50}}{1kpc} \right) \approx \ln(a) + \gamma \ln \left(\frac{M_*}{M_\odot} \right) \quad (2.2)$$

By taking the logarithm of a power law, we end up with an equation for a line. This linear relationship can be seen in figure 2.2. $\ln(a)$ becomes the y-intercept of the line and γ becomes the slope. We have kept denoting this equation as *approximately* equal in order to emphasize that not every galaxy falls exactly into this relationship. However, we can replace that by introducing a galaxy-specific parameter β that is defined to be the galaxy's deviation from this linear relationship.

$$\ln \left(\frac{R_{50}}{1kpc} \right) = \ln(a) + \gamma \ln \left(\frac{M_*}{M_\odot} \right) + \beta \quad (2.3)$$

$$\beta \equiv \ln \left(\frac{R_{50}}{1kpc} \right) - \ln(a) - \gamma \ln \left(\frac{M_*}{M_\odot} \right) \quad (2.4)$$

We will call β the **diffuseness parameter**, because it tells us how diffuse a galaxy is relative to its fellow galaxies. Positive values of β mean that the galaxy has a larger radius than other galaxies of the same mass, and negative values mean a smaller radius. β is especially useful for characterizing the diffuseness because the distribution of β remains

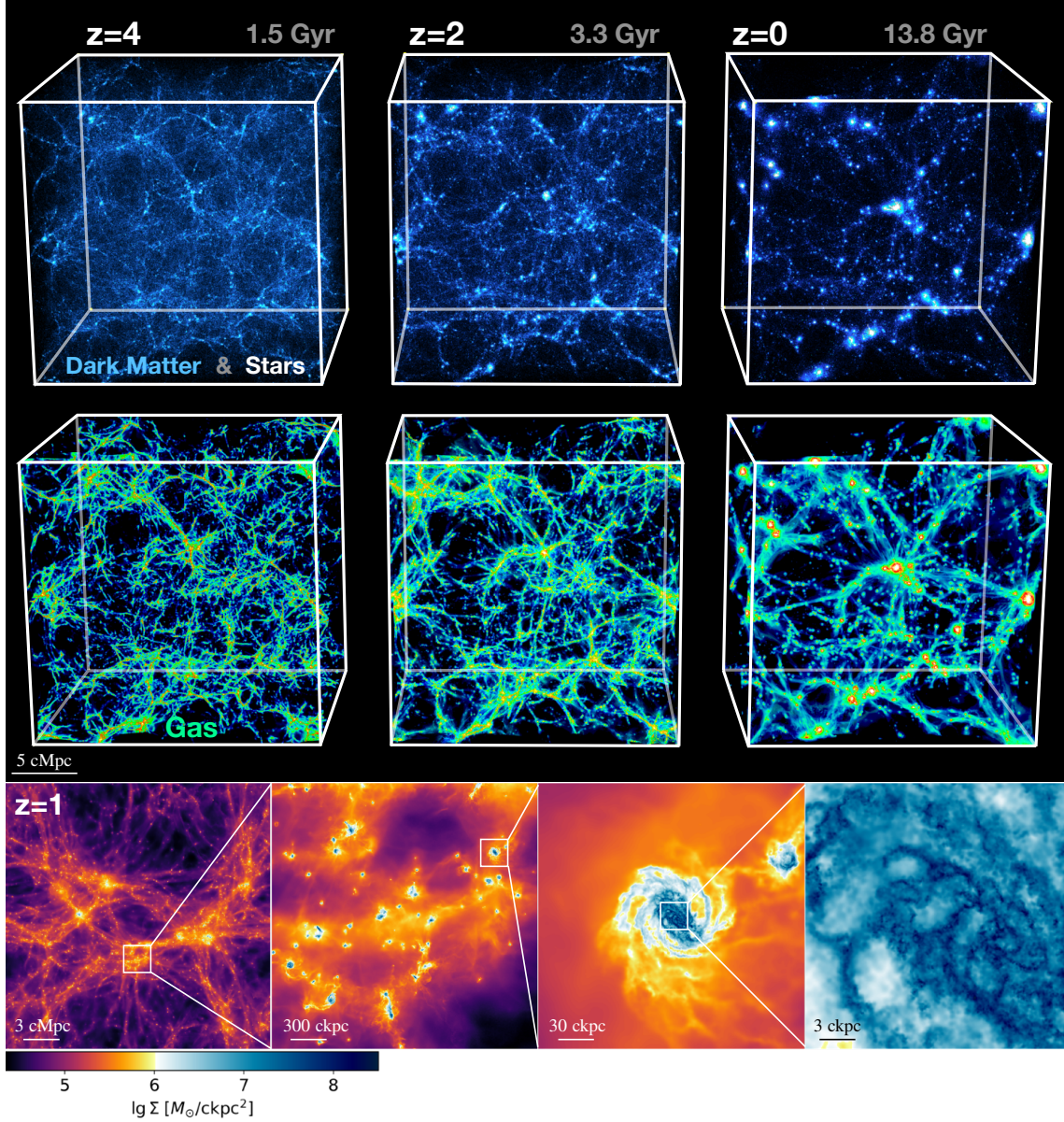
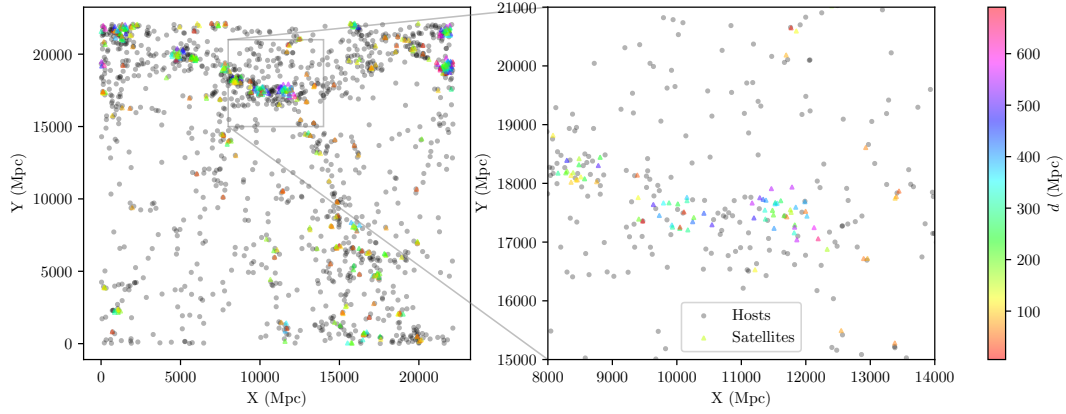


Figure 2.1: From: Feldmann et al. (2022). A representation of the FIREbox simulation. The first two rows depict the state of the simulation at three different time points; the rightmost images depict the simulation in the present time. The top row depicts dark matter in blue and stellar matter in white, while the middle row depicts gas. The bottom row shows a galaxy at different scales within a cluster. As we can see, matter collects into galaxies and systems of galaxies over the course of the simulated universe's evolution. These galaxies take on a variety of sizes, and they share threads of gas and are contained within hierarchical halos of dark matter.



A 2D visualization of FIREbox; the X and Y coordinates of each galaxy. Host galaxies are depicted as gray circles, and satellites galaxies are triangles that are colored by the distance to their host galaxy.

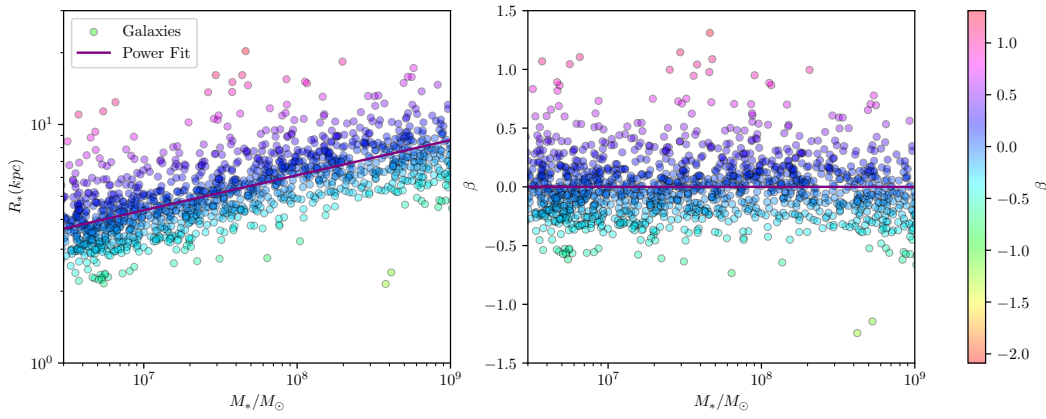


Figure 2.2: The left shows the size-mass relationship for the FIREbox dwarf galaxies. It covers the range $3 \cdot 10^3 - 10^9$. Galaxies larger than this are no longer dwarfs and do not follow the power law, and galaxies smaller than this approach FIREbox's resolution limit. The line of best fit is described by equation 2.2 and β represents the deviation from that line. β is chosen to characterize the diffuseness of a galaxy because the distribution of β is essentially independent of mass, which can be seen in on the right.

consistent across all masses of dwarf galaxies (see figure 2.2). Note that this does not apply for galaxies larger than $10^9 M_\odot$, as they stop following the power law.

We can calculate γ and $\ln(a)$ using equation 2.2 and fitting the dataset to a line. We can then use those values in equation 2.2 to find each galaxy's value of β . We can also characterize the **diversity of the diffuseness** of galaxies using the standard deviation σ_β (the mean is zero by design). We will use these values to compare FIREbox with the galaxies of the Local Group.

2.3 Proximity

To determine what may cause differences in the diffuseness of galaxies, one thing that we may look at is its interactions with its neighbors. Specifically, we will examine a galaxy's distance to its nearest neighbor as well as a satellite galaxy's distance to its host galaxy (as defined by AHF).

Calculating the distance between two galaxies is not as trivial as it may seem because of the shape of FIREbox. The simulation volume is defined as a cube that repeats itself (Feldmann et al., 2022). In other words, if you travel across one border of the universe you appear on the opposite side. This is done to avoid any strange boundary conditions from affecting the simulation, but also without having to simulate an infinite region. In order to measure the X component of the distance between two objects one must first determine whether they are across the X border. If they are, then we find the sum of the distances to the border. Otherwise, we find the difference of their positions like normal. The same logic is used to find the Y and Z components. Only then do we calculate magnitude of the distance.

2.3.1 Minimum Proximity

To determine whether tidal interactions affect the diffuseness of galaxies, it is better to look at the *minimum* distance between a satellite and its host, as opposed to the current distance. The minimum distance is the point at which the tidal forces are strongest, and therefore could cause the most extreme effects. We must therefore also compare β to d_{min} .

Chapter 3

Results and discussion

3.1 Diversity of Dwarf Diffuseness

There are only so many conclusions we can draw about the diversity of dwarf sizes with the given data. The data from McConnachie (2012) spans the range of 10^2 to 10^9 solar masses, with many of the galaxies observed being smaller than $3 \cdot 10^6$. The FIREbox data, however, only covers galaxies greater than $3 \cdot 10^6$. For this reason and others, the lines of best fit defined by $\ln(a)$ and γ (see equation 2.2) for each dataset do not perfectly line up. The diffuseness parameter β is defined relative to the line of best fit for a dataset. It is therefore important to note that the β for individual galaxies across datasets have no meaningful comparison. However, we may still compare the overall diversity of the diffuseness. For FIREbox we have $\sigma_\beta = 0.28$, and for McConnachie (2012) we have a diversity of $\sigma_\beta = 0.66$, over twice as large. The simulated galaxies in FIREbox therefore follow a much stricter size-mass relationship than is expected from real-world observation.

This discrepancy is an example of the diversity of dwarf sizes tension, and Sales et al. (2022) has already shown that it applies to many higher resolution simulations. FIREbox has a larger volume and contains more galaxies than those simulations, and is the first of its size to be detailed enough to resolve low-mass galaxies. It is therefore an important finding that the tension is not resolved in FIREbox, because that is evidence that the tension is *not* caused by a constraint in simulation volume.

3.2 Proximity to Host Galaxy

We find that there is a small correlation between (the logarithm of) a satellite's distance to its host galaxy and its diffuseness (see figure 3.1). This correlation is approximately the same regardless of whether we measure the absolute separation or Virial separation: $r = .22$, $p \leq .001$ for the former and $r = .26$, $p \leq .001$ for the latter. As we can see in the figures, the data is essentially untouched except for the galaxies of low dark matter with $d/R_{vir} < 0.2$. Below this threshold, as Moreno et al. (2022) establishes, a satellite galaxy experiences a

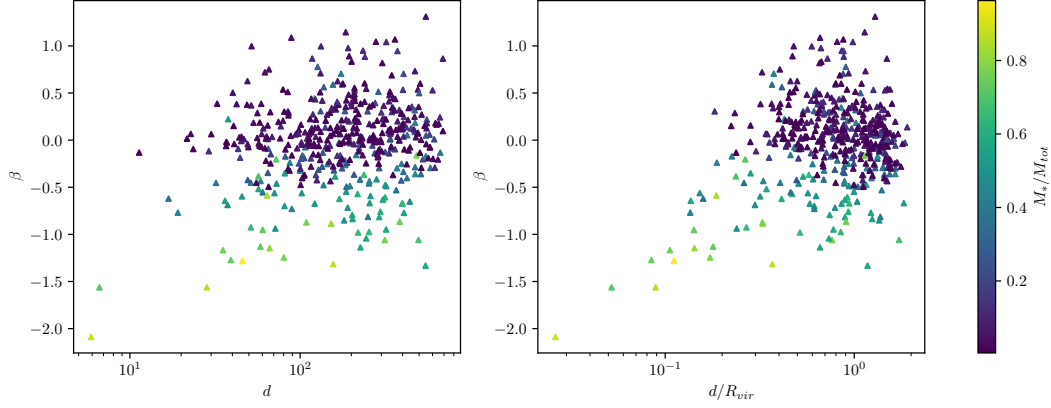


Figure 3.1: Shows the diffuseness of satellites as a function of distance to their host galaxies. On the left, it compares the absolute separation. On the right, it shows the Virial separation (distance as a fraction of the host galaxy’s Virial radius). The correlation for these is small: $r = .22, p \leq .001$ for d and $r = .26, p \leq .001$ for d/R_{vir} . This slight positive correlation in both sets of parameters is likely caused by the dark matter deficient galaxies (shown in light green and yellow), whose outer regions are likely tidally disrupted, leaving only a core.

level of tidal disruption that either disassembles it entirely forms a dark matter deficient galaxy. However, above this threshold there appears to not be much of an effect. In fact, if we exclude galaxies below this critical threshold from our analysis, we find that there is absolutely no correlation: $r = .06, p = .23$ for absolute distance and $r = -.03, p = .51$ for Virial separation. We may therefore conclude that a variance in proximity to a host galaxy is not responsible for the diversity of diffuseness in galaxies.

3.3 Minimum Proximity

When we plot the diffuseness of a satellite against the minimum separation between it and its host, we find an uneven distribution (see figure 3.2). A majority of galaxies are clustered towards the right, and only a few outliers are towards the bottom left. However, we notice that these outliers are the dark matter deficient galaxies. Including the outliers gives us no correlation for these parameters: $r = .04, p = .51$ for d and $r = -0.07, p = .25$ for d_{min}/R_{vir} .

However when we exclude galaxies with $d_{min} \leq 0.2R_{vir}$, we get a much different picture. While there is no correlation for the absolute distances ($r = -0.03, p = .62$) there is a medium negative correlation between β and d_{min}/R_{vir} : $r = -0.32, p \leq .001$.

3.4 Proximity to Nearest Neighbor

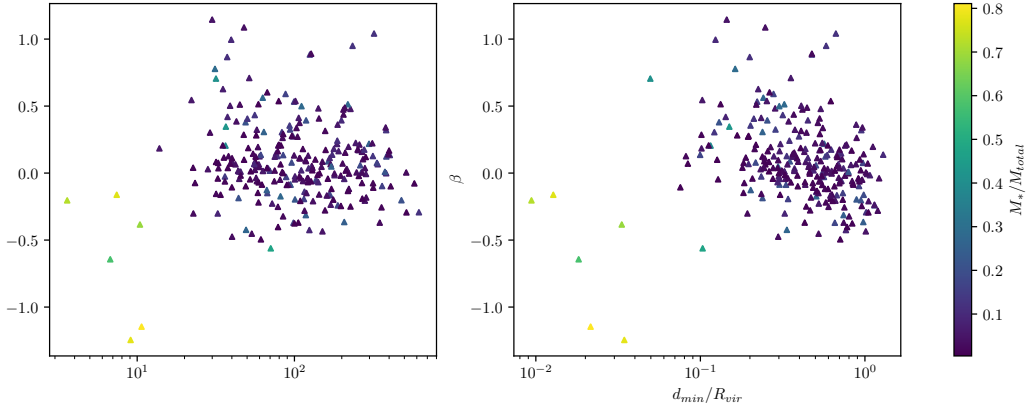


Figure 3.2: Shows the diffuseness of satellites as a function of minimum distance to their host galaxies. On the left, it compares the absolute separation. On the right, it shows the Virial separation. There is no correlation for these parameters: $r = .04$, $p = .51$ for d_{min} and $r = -0.07$, $p = .25$ for d_{min}/R_{vir} .

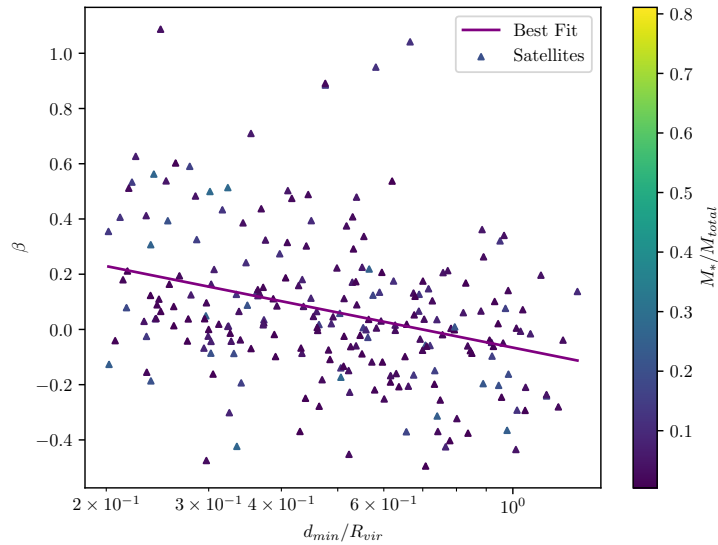


Figure 3.3: A zoom-in of figure 3.2 showing the diffuseness of satellite galaxies as a function of their minimum Virial separation. This graph only includes galaxies above the critical separation of $0.2R_{vir}$, below which a galaxy would either be entirely destroyed or converted into a dark matter deficient galaxy. There is a medium negative correlation between these parameters: $r = -0.32$, $p \leq .001$

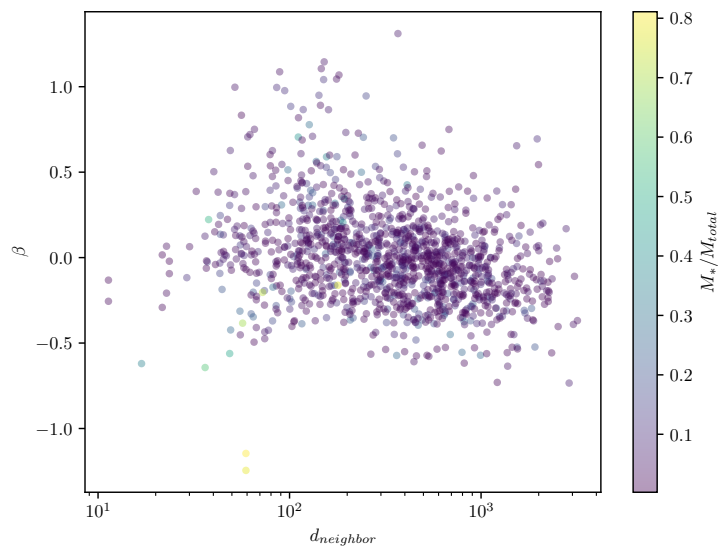


Figure 3.4: Shows a galaxy's distance to its nearest neighbor. There is a slight negative correlation between these parameters: $r = .26$, $p \leq .001$. We

Chapter 4

Conclusions and future work

4.1 Size-mass-proximity relation

We discovered that β is correlation with the log of a satellite's proximity to its host galaxy. This relationship, as we will demonstrate, implies that we can include this distance as a new term in the formula for the size-mass relationship (equation 2.2). To prove this, we will reverse engineer that equation starting from equation 2.2. We will begin by expressing β in terms of d_{min}/R_{vir} using the experimental results found in figure 3.3.

$$\beta = -0.18 \ln \left(\frac{d_{min}}{R_{vir}} \right) \quad (4.1)$$

Where -0.18 is the slope of the line of best fit in this relationship. We can plug this into equation 2.2, giving us

$$\ln \left(\frac{R_{50}}{1kpc} \right) = \ln(a) + \gamma \ln \left(\frac{M_*}{M_\odot} \right) - 0.18 \ln \left(\frac{d_{min}}{R_{vir}} \right) \quad (4.2)$$

We take the exponent to reveal the final power law relationship.

$$R_{50} = a \left(\frac{M_*}{M_\odot} \right)^\gamma \left(\frac{d_{min}}{R_{vir}} \right)^{-0.18} kpc \quad (4.3)$$

And finally, we may plug in the experimental values of a and γ (see figure 2.2). This gives us a final equation of

$$R_{50} = 0.41 \left(\frac{M_*}{M_\odot} \right)^{0.15} \left(\frac{d_{min}}{R_{vir}} \right)^{-0.18} kpc \quad (4.4)$$

As we can see, a satellite's distance to its host has just as much of an influence on its radius as its mass does.

4.2 Further Work

Bibliography

- L. V. Sales, A. Wetzel, and A. Fattahi, *Nature Astronomy* **6**, 897 (2022), ISSN 2397-3366.
- A. W. McConnachie, *The Astronomical Journal* **144**, 4 (2012), ISSN 1538-3881.
- R. Feldmann, E. Quataert, C.-A. Faucher-Giguère, P. F. Hopkins, O. Çatmabacak, D. Kereš, L. Bassini, M. Bernardini, J. S. Bullock, E. Cenci, et al., *FIREbox: Simulating galaxies at high dynamic range in a cosmological volume* (2022), arXiv:2205.15325.
- V. De Luca and J. Khouri, *Superfluid Dark Matter around Black Holes* (2023), arXiv:2302.10286.
- A. Bassi, S. A. Adil, M. P. Rajvanshi, and A. A. Sen, *Cosmological Evolution in Bimetric Gravity: Observational Constraints and LSS Signatures* (2023), arXiv:2301.11000.
- F. Bournaud, B. G. Elmegreen, R. Teyssier, D. L. Block, and I. Puerari, *Monthly Notices of the Royal Astronomical Society* **409**, 1088 (2010), ISSN 0035-8711.
- P. F. Hopkins, A. Wetzel, D. Kereš, C.-A. Faucher-Giguère, E. Quataert, M. Boylan-Kolchin, N. Murray, C. C. Hayward, S. Garrison-Kimmel, C. Hummels, et al., *Monthly Notices of the Royal Astronomical Society* **480**, 800 (2018), ISSN 0035-8711.
- A. Fitts, M. Boylan-Kolchin, O. D. Elbert, J. S. Bullock, P. F. Hopkins, J. Oñorbe, A. Wetzel, C. Wheeler, C.-A. Faucher-Giguère, D. Kereš, et al., *Monthly Notices of the Royal Astronomical Society* **471**, 3547 (2017), ISSN 0035-8711.
- C. Wheeler, P. F. Hopkins, A. B. Pace, S. Garrison-Kimmel, M. Boylan-Kolchin, A. Wetzel, J. S. Bullock, D. Kereš, C.-A. Faucher-Giguère, and E. Quataert, *Monthly Notices of the Royal Astronomical Society* **490**, 4447 (2019), ISSN 0035-8711.
- J. Moreno, S. Danieli, J. S. Bullock, R. Feldmann, P. F. Hopkins, O. Catmabacak, A. Gurvich, A. Lazar, C. Klein, C. B. Hummels, et al., *Nature Astronomy* **6**, 496 (2022), ISSN 2397-3366, 2202.05836.
- E. Applebaum, A. M. Brooks, C. R. Christensen, F. Munshi, T. R. Quinn, S. Shen, and M. Tremmel, *The Astrophysical Journal* **906**, 96 (2021), ISSN 0004-637X.
- S. R. Knollmann and A. Knebe, *The Astrophysical Journal Supplement Series* **182**, 608 (2009), ISSN 0067-0049.

Appendix A

Calculating distances in FIREbox

...